Membrane Fusion Mediated by the Influenza Virus Hemagglutinin Requires the Concerted Action of at Least Three Hemagglutinin Trimers

Tsafi Danieli,[‡§] Sandra L. Pelletier,[*] Yoav I. Henis,[§] and Judith M. White[*‡]

[*]Department of Cell Biology, University of Virginia, Health Sciences Center, Charlottesville, Virginia 22908;
[‡]Department of Pharmacology, University of California, San Francisco, California 94143; and
[§]Department of Neurobiochemistry, George S. Wise Faculty of Life Sciences, Tel Aviv University, Tel Aviv 69978 Israel

Abstract. In this study we tested the hypothesis that fusion mediated by the influenza virus hemagglutinin (HA) is a cooperative event. To do this we characterized 3T3 cell lines that express HA at nine different defined surface densities. HA densities ranged from 1.0 to 12.6×10^3 HA trimers/μm^2 as determined by quantitative fluorescent antibody binding. The lateral mobility and percent mobile fraction of HA did not vary significantly among these cells, nor did the contact area between HA-expressing cells and target RBCs. The fusion reaction of each HA-expressing cell line was analyzed using a fluorescence dequenching assay that uses octadecylrhodamine (R18)-labeled RBCs. For each cell line we measured the lag time preceding the onset of fusion, the initial rate of fusion, and the final extent of fusion. The final extent of fusion was similar for all cell lines, and the initial rate of fusion as a function of HA surface density displayed a Michaelis-Menten–type dependence. However, the dependence of the lag time preceding the onset of fusion on HA surface density was clearly sigmoidal. Kinetic analysis of the data for the reciprocal lag time vs HA surface density, by both a log/log plot and a Hill plot, suggested that the observed sigmoidicity does not reflect cooperativity at the level of formation of HA aggregates as a prerequisite to fusion. Rather, the cooperativity of the process(es) that occur(s) during the lag time arises at a later step and involves a minimum of three, and most likely four, HA trimers. A model is proposed to explain HA cooperativity during fusion.

MEMBRANE fusion is a fundamental biological process that proceeds via the formation of a fusion pore (Lindau and Almers, 1995; Monck and Fernandez, 1992; White, 1992, 1994; Zimmerberg et al., 1993). A fusion pore is defined as the first aqueous connection between two fusing compartments. Exocytic fusion pores have been characterized extensively by high resolution electrophysiological techniques (Lindau and Almers, 1995; Monck and Fernandez, 1992; Zimmerberg et al., 1993). Similar approaches have recently been applied to study fusion mediated by the influenza virus hemagglutinin (HA)[1] (Melikyan et al., 1993*a*, *b*; Spruce et al., 1991, 1989; Tse et al., 1993; Zimmerberg et al., 1994). The latter studies have shown that the fusion pores that form during HA-mediated fusion share many characteristics with exocytic fusion pores, notably a small (~1–2 nm) estimated initial diameter (Spruce et al., 1991).

Although many of the constituents that participate in exocytic and other intracellular fusion events have recently been discovered (Bennett and Scheller, 1994; Ferro-Novick and Jahn, 1994; Pryer et al., 1992; Rothman, 1994; Südhof et al., 1993), neither the minimal number of proteins that comprise the exocytic fusion pore nor the molecular mechanism of exocytic fusion is yet known. In contrast, it is well documented that the influenza HA is both necessary and sufficient for membrane fusion (Stegmann et al., 1989; White, 1992, 1994). Moreover, a great deal is known about the structure of HA and its fusion mechanism (Bullough et al., 1994; Hughson, 1995; Stegmann and Helenius, 1993; White, 1994; Wiley and Skehel, 1987). HA is a homotrimer in which each monomer consists of two disulfide-bonded subunits. The HA1 subunit houses the receptor binding domain. The HA2 subunit houses the fusion peptide, a protein segment critical for fusion activity (Gething et al., 1986). After binding to receptors on target membranes, HA initiates fusion in response to low pH , a condition that influenza virus experiences in the endoso-

Address all correspondence to Judith M. White, Department of Cell Biology, University of Virginia, Box 439, Charlottesville, VA 22908. Tel.: (804) 924-2593. Fax: (804) 982-3912.

1. *Abbreviations used in this paper*: D, lateral diffusion coefficient; FPR, fluorescence photobleaching recovery; HA, influenza virus hemagglutinin; NaBut, sodium butyrate; NBD-PE, NBD-labeled phosphatidylethanolamine; TMR, tetramethylrhodamine.

mal compartment. Below a threshold pH, HA changes conformation, exposes its fusion peptides, and binds hydrophobically to target bilayers. The next stages of the fusion reaction are less clear but appear to involve a hemifusion intermediate (Kemble et al., 1994; Melikyan et al., 1995), the opening of a narrow fusion pore, and dilation of the fusion pore (Melikyan et al., 1993*a*,*b*; Spruce et al., 1991, 1989; Tse et al., 1993; Zimmerberg et al., 1994).

Since HA is both necessary and sufficient for membrane fusion, models have been proposed in which the HA fusion pore is lined with several conformationally altered HA trimers (Bentz et al., 1990; Ellens et al., 1990; Guy et al., 1992; Stegmann et al., 1990; White, 1992, 1994). Support for the concept that HA-mediated fusion is a cooperative process has come from several lines of indirect evidence: (*a*) the curve relating the initial rate of fusion and pH is steep (Morris et al., 1989); (*b*) for two cell lines whose HA surface density varies by a factor of 1.6, the extent of fusion varies by a factor of 4.4 (Ellens et al., 1990); (*c*) images consistent with aggregates of two to three HA trimers have been seen on low pH-treated virus particles (Doms and Helenius, 1986). Although suggestive, none of these findings have provided proof for HA cooperativity, nor have they indicated the minimum number of HA trimers required.

As described for other systems (Cooper et al., 1983), proof that HA-mediated fusion is a cooperative event requires analysis of the fusion reactions of membranes that express HA at different defined surface densities. In this study we conducted such an analysis. We characterized in detail the fusion reactions of NIH 3T3 fibroblasts that express influenza HA trimers at nine different defined surface densities. Our results indicate that HA-mediated fusion is indeed a cooperative process. Moreover, they suggest that a minimum of three, and most likely four, HA trimers is required to initiate a fusion reaction.

Materials and Methods

Materials

Octadecylrhodamine B chloride (R18) and NBD-labeled phosphatidylethanolamine (NBD-PE) were obtained from Molecular Probes, Inc. (Eugene, OR). *N*-1-tosylamide-2-phenylethylchloromethyl ketone–treated trypsin, soybean trypsin inhibitor, neuraminidase (from *Clostridium perfringens*), and RPMI medium were obtained from Sigma Chemical Co. (St. Louis, MO). Supplemented calf serum was obtained from either Hyclone Laboratories, Inc. (Logan, UT) or from the University of California at San Francisco (UCSF) tissue-culture facility. Other tissue-culture reagents were purchased from either the UCSF or the University of Virginia tissue-culture facilities. Polyclonal rabbit antiserum against the HA protein of A/Japan/305/57 was kindly provided by Dr. Michael Roth (University of Texas Southwestern Medical Center, Dallas, TX). Monovalent Fab′ fragments labeled with tetramethylrhodamine (TMR)–isothiocyanate (TMR-Fab′) were prepared as described (Gutman et al., 1993).

Cell Lines

Six NIH 3T3 cell lines expressing different amounts of HA from the Japan strain of influenza virus (A/Japan/305/57) were isolated from a cell line (BV1-MTHA/NIH) obtained by transfection of 3T3 cells with Japan HA cDNA (Sambrook et al., 1985). Two cell lines, gp4 (Gething, M.-J., and J. Sambrook, unpublished observations) and HA-b (Doxsey et al., 1985), were isolated based on their ability to bind fluorescently labeled RBCs using strictly analogous procedures. Single cell clones were isolated from these HA-expressing cell lines by plating the cells at 50 cells per 100-mm dish and picking random clones. After an additional round of single cell cloning, clones were selected for their ability to bind RBCs, to remain adherent to tissue-culture plastic throughout the preparations for RBC binding and fusion, and then for expression of different levels of HA based on a radioimmunoassay (Gething et al., 1986). Selection of the gp4f (alternatively called GP4F) and HAb-2 clones was described previously (Ellens et al., 1990). Four additional clones, gp4/6, gp4/10, gp4/9, and gp4/8, were subcloned from the gp4 cells using the same procedures. To obtained increased HA expression, HAb-2 cells, the line expressing the most HA, were treated with sodium butyrate (NaBut); 3 d after plating, and 18 h before fusion experiments, the HAb-2 cells were fed with growth medium containing 1.0, 3.0, or 5.0 mM NaBut. In specified experiments, gp4f cells were treated similarly with 5.0 mM NaBut. NaBut treatment did not affect cell size as determined by light scattering analysis.

Determination of Relative HA Surface Density and Lateral Mobility

For measurements of HA surface density and lateral mobility, cells were grown on glass coverslips. 2 d after plating, the cells were washed twice with HBSS devoid of phenol red and bicarbonate (Biological Industries, Beth Haemek, Israel) and supplemented with 20 mM Hepes and 2% BSA at pH 7.2 (HBSS/Hepes/BSA). They were then incubated in the same buffer with anti-HA TMR-Fab′ fragments (100 μg/ml) for 45 min at 4°C. The HA-expressing cells were then rinsed three times in label-free buffer, mounted over a serological slide containing a well filled with HBSS/Hepes/BSA, and used for fluorescence photobleaching recovery (FPR) experiments or for determination of the relative HA density at the cell surface. Lateral diffusion coefficients (D) and mobile fractions of TMR-Fab′–labeled HA proteins were measured by FPR (Axelrod et al., 1976; Koppel et al., 1976) with an apparatus described previously (Henis and Gutman, 1983). All measurements were conducted at 22°C within 30 min after labeling, conditions under which endocytosis of HA is negligible (Fire et al., 1991). The monitoring laser beam (Innova 70 argon ion laser, 529 nm, 1 μW; Coherent Inc., Palo Alto, CA) was focused through a microscope (Zeiss Universal; Carl Zeiss, Inc., Thornwood, NY) to a Gaussian radius of 1 μm using a ×100 objective. A brief pulse (5 mW, 30 ms) bleached 50–70% of the fluorescence in the illuminated region. The time course of the fluorescence recovery was followed by the attenuated monitoring beam. D and mobile fractions were extracted from the fluorescence recovery curves by nonlinear regression analysis (Petersen et al., 1986). Incomplete fluorescence recovery was interpreted to represent fluorophores that are immobile on the time scale of the FPR experiment ($D \leq 5 \times 10^{-12}$ cm^2/s). Quantitative measurements of HA surface density were carried out using the FPR instrumentation, except that the laser beam was always attenuated (nonbleaching conditions) and a ×40 objective (yielding a beam with 1.46-μm Gaussian radius) replaced the ×100 objective, thereby covering a sixfold larger area of cell surface. The response of the photomultiplier tube was linear over the entire range of fluorescence intensities measured (expressed in arbitrary fluorescence units). The cell line expressing the lowest amount of HA, gp4/6, was used as a reference to which the other cell lines were compared.

Determination of Relative HA Density by Surface Biotinylation

Cells (gp4f and 5 mM NaBut-induced gp4f) were treated with trypsin and neuraminidase as described in the next section. The cells were then chilled and treated with NHS-LC-Biotin, a membrane-impermeable biotinylating reagent, essentially as described (Kemble et al., 1993). After biotinylation, the cells were either stored at -20°C for future analysis (after scraping from dishes, pelleting, washing, and repelleting) or lysed directly on dishes. Cells from one 10-cm plate were lysed at room temperature in 1 ml of lysis buffer, pH 7.5, containing 1% NP-40, 50 mM Hepes, and the following protease inhibitors: 1 mM PMSF, 1 μg/ml pepstatin A, 2 μg/ml leupeptin, 4 μg/ml aprotinin, 10 μg/ml antipain, 50 μg/ml benzamidine, 10 μg/ml soybean trypsin inhibitor, 0.5 mM iodoacetamide. The lysate was centrifuged at 15,000 *g* in an Eppendorf microfuge for 20 min (Eppendorf North America, Inc., Madison, WI). Samples of cleared cell lysates containing equal total protein (70–100 μg), as determined with the bicinchoninic acid reagent (Pierce Chemical Co., Rockford, IL), were subjected to immunoprecipitation with 5 μg of polyclonal IgG directed against HA from the Japan strain of influenza virus essentially as described (Kemble et al., 1993). Immunocomplexes were suspended in SDS–gel loading buffer, pH 7.5, containing 62.5 mM Tris, 2% SDS, 7.5% sucrose, 0.5 mM EDTA, 0.005% bromophenol blue, and 100 mM DTT, heated to 95°C for

5 min, separated on a nonreducing 12.5% SDS–polyacrylamide gel, and transferred to nitrocellulose (Schleicher and Schuell, Inc., Keene, NH). The nitrocellulose was blocked with PBS containing 3% skim milk, 10% glycerol, 1% BSA, 18% glucose, and 0.5% Tween 20. The blots were washed several times with PBS containing 0.5% Tween 20, and then probed with 10 μCi of ^{125}I-streptavidin in PBS containing 0.5% Tween 20, 18% glucose, 10% glycerol, and 1% BSA. The filters were then subjected to phosphorimage analysis using a PhosphorImager workstation (Molecular Dynamics, Sunnyvale, CA). Intensities of the HA1 and HA2 bands were summed.

Preparation, Binding, and Fusion of R18-labeled RBCs

Freshly drawn RBCs (1% hematocrit) were washed and labeled with R18 as described previously (Kemble et al., 1992; Morris et al., 1989). R18-labeled RBCs were washed two times with RPMI containing 10% supplemented calf serum, washed four times with RPMI, and then resuspended in 10 ml RPMI. Labeled RBCs were stored at 4°C in the dark and used within 6 d. Binding of R18-labeled RBCs to HA-expressing cells was performed essentially as described previously (Kemble et al., 1992) except that the binding solution contained 0.025–0.03% (vol/vol) RBCs (unless otherwise stated), and that binding was conducted for 20 min at 25°C. Fusion of R18-labeled RBCs was performed as described previously (Kemble et al., 1992) in a thermostatted cuvette at 28° to 29°C. Fluorescence measurements were made on a fluorimeter equipped with a magnetic stirrer (LS-5B; Perkin-Elmer, San Jose, CA). For all fusion experiments, the fibroblasts were pretreated with trypsin to cleave the fusion-inactive precursor (HA0) to its fusion active (HA1-S-S-HA2) form as described previously (Kemble et al., 1992). Fibroblasts expressing HA0 displayed no fluorescence dequenching, as shown previously (Morris et al., 1989).

Observation of the Contact Area between RBCs and HA-expressing Cells

HA-expressing cells were washed with RPMI and incubated with the fluorescent probe NBD-PE at a final concentration of 150 μM in RPMI containing 50 mM glucose at 4°C for 20 min. The cells were then washed with RPMI containing 10% supplemented calf serum and incubated with 0.03% (vol/vol) R18-labeled RBCs. The RBC–cell complexes were washed and removed from their dishes with 0.5 mM EDTA/0.5 mM EGTA in PBS, placed on a glass slide, and observed with a confocal microscope (Bio-Rad Laboratories, Cambridge, MA). During all stages of labeling and RBC binding, the HA-expressing fibroblasts were kept at 4°C to minimize endocytosis of the lipid probe.

Hill Plot Analysis

The Hill equation, used to describe cooperative systems (Levitzki, 1978), is given by:

$$\log (Y/1 - Y) = \log K + n\log [S] , \quad (1)$$

where Y is the saturation function (equivalent to v/V_{max} in steady-state kinetics), K is a constant (equivalent to the overall association constant for binding equilibria), and $[S]$ is the concentration of the species that shows the cooperative phenomenon. A plot of log (Y/1-Y) (or an equivalent expression) vs. log $[S]$, a Hill plot, yields the Hill coefficient, n_H, which is the slope at midsaturation. It is important to note that at the low and high ends of $[S]$, the Hill plot for cooperative systems tends to deviate from linearity and the slope (n) approaches 1 (Levitzki, 1978). In the case of HA-mediated fusion, the reciprocal of the lag time (1/lag) is proportional to the rate of the process that precedes fusion. Hence, it is possible to substitute 1/lag for Y in the Hill plot to evaluate the cooperativity of HA-mediated fusion, provided that the 1/lag values are calibrated such that the highest value (at saturation, where elevating HA density no longer affects the lag time) is assigned the value of 1. In this way, the 1/lag values equal those of the saturation function, Y.

Results

The present study had two goals: to determine whether the process of HA-mediated membrane fusion is a cooperative event, and, if so, to estimate the minimum number of HA trimers involved. Toward these goals, we isolated and characterized a series of cell lines that vary in the density of HA trimers on their surfaces. We then examined their fusion reactions with RBCs in detail using a fluorescence dequenching assay. Finally, we compared the lag times preceding the onset of fusion, the initial rates of fusion, and the final extents of fusion among all of the cell lines.

Density of HA in the Plasma Membrane

For our analysis we used subclones of an NIH 3T3 cell line expressing HA from the Japan strain (A/Japan/307) of influenza virus (Sambrook et al., 1985). Two of the cell lines, gp4f and HAb-2, were characterized previously (Ellens et al., 1990). Four additional subclones, gp4/6, gp4/8, gp4/9, and gp4/10, were selected for expression of different amounts of HA at their surfaces as described in the Materials and Methods section. To obtain higher HA expression levels, the cell line expressing the highest amount of HA, HAb-2, was treated with 1.0, 3.0, or 5.0 mM NaBut. The relative amount of HA expressed at the surface of each cell line was then determined by quantitative fluorescent Fab′ antibody binding as described in the Materials and Methods section (Table I). The actual expression levels were calculated with reference to the density of HA on the surface of the gp4f cell line. The density of HA at the surface of gp4f cells, 1.6×10^3 HA trimers per μm^2, was determined previously using an HA radioimmunoassay in

Table I. Characterization of Cell Lines Expressing Different Surface Densities of HA

Cell line	NaBut	Fluorescence	HA/μm^2	Relative density	D	Mobile fraction
	mM	*AU*			*cm^2/s × 10^{-10}*	%
gp4/6		1,225 ± 83	0.98×10^3	1.0	3.6 ± 0.3	67 ± 4
gp4/10		1,633 ± 63	1.28×10^3	1.3		
gp4f		2,016 ± 78	1.60×10^3	1.6	3.0 ± 0.3	72 ± 3
gp4/9		2,059 ± 114	1.71×10^3	1.7		
gp4/8		2,940 ± 255	2.34×10^3	2.4		
HAb-2		3,167 ± 119	2.51×10^3	2.6	3.0 ± 0.4	66 ± 3
HAb-2	1	4,288 ± 241	3.44×10^3	3.5		
HAb-2	3	4,655 ± 302	3.74×10^3	3.8		
HAb-2	5	15,680 ± 354	12.60×10^3	12.8	2.3 ± 0.2	71 ± 3

Cell labeling with TMR-Fab′ and mobility measurements were performed as described in the Materials and Methods section. Fluorescence intensity is expressed in arbitrary units (AU). 30–50 cells were measured for each cell line. Results are given as mean ± SEM. For the NaBut-induced cells, the fluorescence intensity measurements were conducted in three separate experiments for each NaBut concentration, yielding results that differed by <15%.
*Relative density with respect to HA density in the gp4/6 cell line.

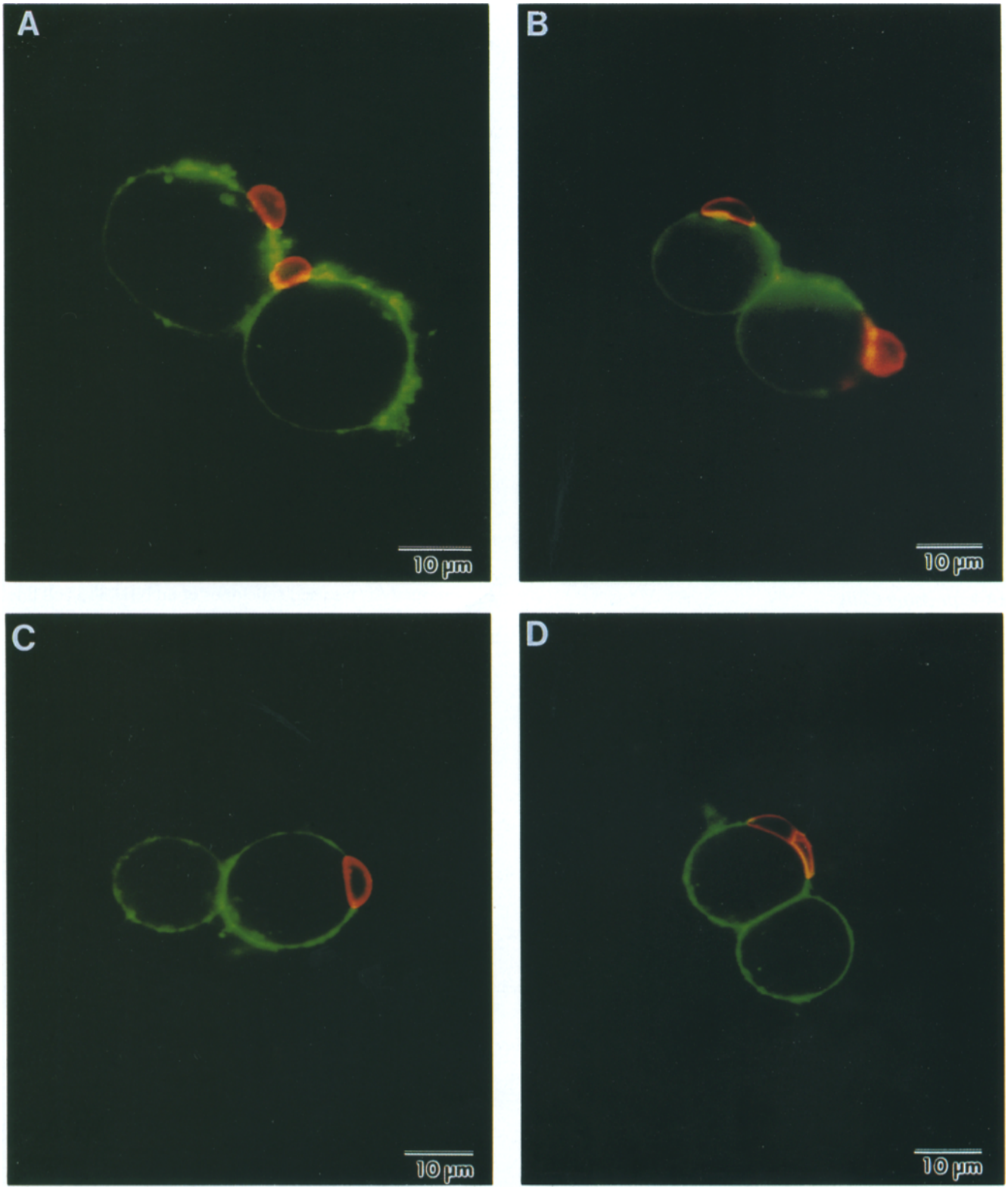

Figure 1. Binding of R18-labeled RBCs to representative HA-expressing cell lines. HA-expressing cells (see Table I) were labeled with the fluorescent dye NBD-PE and then incubated with R18-labeled RBCs. After washing, the RBC–cell complexes were observed with a confocal microscope. The cells analyzed were: (*A*) gp4/6, (*B*) gp4f, (*C*) HAb-2, and (*D*) 5 mM NaBut-induced HAb-2. For all cells, the long axis of the attachment site with RBCs is similar: ~7.1 μm. Procedural details are described in the Materials and Methods section.

conjunction with capacitance measurements of the cell surface area (Ellens et al., 1990). Based on the present analysis, the HA cell surface expression levels among the set of cells analyzed varied over a nearly 13-fold range, from 0.98×10^3 to 12.6×10^3 HA trimers per μm^2 (Table I).

HA is expressed on the surface of fibroblasts in its fusion-inactive precursor (HA0) form. As shown previously (Gething et al., 1986), treatment with 5 μg/ml trypsin cleaved virtually all of the cell surface HA0 in all of the cell lines to the fusion-competent form consisting of the two disulfide-bonded subunits, HA1 and HA2 (not shown).

Mobility of HA in the Plasma Membrane

The HA at the surface of all of the HA-expressing cell lines analyzed to date is highly mobile in the plane of the membrane (Ellens et al., 1990; Gutman et al., 1993). To exclude the possibility that different expression levels of HA caused a major effect on HA lateral mobility, we performed FPR measurements on four representative cell lines: gp4/6, gp4f, HAb-2, and 5 mM NaBut-induced HAb-2. The surface expression levels of HA in these four cell lines covered the entire range of HA surface densities analyzed (Table I). In all four representative cell lines, HA displayed high and similar lateral mobilities: D, $\sim 3 \times 10^{-10}$ cm^2/s with mobile fractions of ~70% (Table I). For the two cell lines that displayed the lowest and highest levels of HA at their surfaces, gp4/6 and 5 mM NaBut-induced HAb-2, the D values differed by a factor of only 1.5. This result is in accord with a previous study on the EGF receptor indicating a weak dependence for the lateral mobility of membrane proteins on their surface density (Benveniste et al., 1988).

Contact Area between HA-expressing Cells and RBCs

We next measured the contact areas between cells expressing different levels of HA and bound RBCs, as differences in this parameter might affect fusion kinetics. To do this, the plasma membrane of HA-expressing cells was labeled with a fluorescent phospholipid probe, NBD-PE. The HA-expressing fibroblasts were then incubated with a 0.03% solution of R18-labeled RBCs for 20 min at 4°C. This concentration of RBCs was chosen, as it led to the binding of, on average, one to three RBCs to all of the HA-expressing cells described in Table I, including those treated with NaBut. Moreover, this level of RBC binding proved optimal for fusion experiments (see below). The HA-expressing cell–RBC complexes were then examined by confocal microscopy. Images of RBCs bound to fibroblasts from the four representative HA cell lines, gp4/6, gp4f, HAb-2, and 5 mM NaBut-induced HAb-2, covering the range of HA expression levels studied, are shown in Fig. 1. To estimate the size of the attachment region between RBCs and the HA-expressing cells, we focused on cells where the RBCs were seen in side view and chose the focal depth yielding the longest contact region between the RBC and the fibroblast. The long axis of this region was measured for 20 RBC–cell complexes for each HA-expressing cell line. Based on this analysis, the average length of the attachment site was 7.1 μm for all cell lines, with a standard error, in all cases, of 0.20–0.25 μm. If the contact area is modeled as a circle, this represents an attachment area of 38 μm^2. For all cell lines the contact area was the same for each RBC bound, regardless of whether there were one, two, three, or four RBCs bound per HA-expressing fibroblast.

Parameters of the Fusion Assay

The fluorescence dequenching fusion assay is based on dilution of the R18 probe from RBCs into the larger HA-expressing fibroblasts. To observe dequenching in all cells, the assay requires that, on average, at least one RBC bind and fuse per fibroblast. However, if too many RBCs fuse per cell, there will be incomplete dequenching due to inadequate dilution of the probe. We therefore analyzed the effect of varying the concentrations of added RBCs on the lag phase preceding the onset of fusion and on the initial rate and final extent of fusion as measured by the fluorescence dequenching assay.

HAb-2 cells were incubated with 0.02–0.05% RBCs and washed as described in the Materials and Methods section. After incubation with 0.02% RBCs, ~80% of the HA-expressing cells displayed one to three RBCs bound per cell. After incubation with 0.03% RBCs, ~80% of the cells displayed two to five RBCs bound per cell. As shown in Fig. 2, HAb-2 cells that had been incubated with 0.02% labeled RBCs (i.e., with one to three RBCs bound) displayed a faster rate of fluorescence dequenching than HAb-2 cells incubated with 0.03% labeled RBCs (i.e., with two to five RBCs bound). In addition, cells with one to

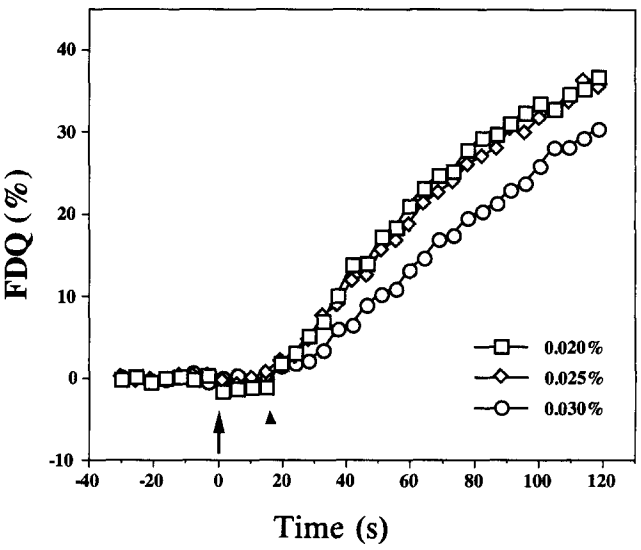

Figure 2. Effect of RBC concentration on the fusion of HAb-2 cells with R18-labeled RBCs as monitored by R18 fluorescence dequenching. RBCs were labeled with R18 and bound to HA-expressing cells, and the RBC–cell complexes were assayed for fluorescence dequenching at 28° to 29°C as described in the Materials and Methods section. The 0 time point (*arrow*) represents the time of lowering the pH to 5.0. The arrowhead denotes the onset of fluorescence dequenching. The lag phase is defined as the time between the arrow and the arrowhead. The final percentages of fluorescence dequenching were 48 and 47%, respectively, for fibroblasts incubated with 0.02% and 0.025% labeled RBCs, and 35% for fibroblasts incubated with 0.03% labeled RBCs. Data shown are for the HAb-2 cell line. Virtually identical patterns were obtained for all of the HA-expressing cells tested.

three RBCs bound showed a higher final extent (~45%) of fluorescence dequenching than that observed (~35%) for cells with two to five RBCs bound. Incubating with still higher concentrations of RBCs (0.05%; 5–10 RBCs bound per cell) resulted in an even slower initial rate and a lower (~25%) final extent of fluorescence dequenching (not shown). These results most likely reflect inadequate dilution of the probe when too many RBCs fuse per cell. However, and importantly, over the range of concentrations of added RBCs used in this study, 0.02–0.03%, the lag phase preceding the onset of fluorescence dequenching did not vary (Fig. 2). The lag phase also did not vary when even higher concentrations of RBCs, 0.05%, were added (not shown). All of the cell lines described in Table I (including NaBut-induced HAb-2s) bound, on average, the same number of RBCs for a given concentration of RBCs added. In addition, similar fluorescence profiles to those displayed in Fig. 2 were obtained for all HA-expressing cell lines analyzed.

Fusion of RBCs with Cell Lines That Express Different Amounts of HA at Their Surface

The fusion reactions of the four representative HA-expressing cell lines depicted in Fig. 1 with R18-labeled RBCs were analyzed using the fluorescence dequenching assay (Fig. 3). For this analysis, the concentration of added RBCs was 0.02%, as this concentration yielded, on average, one to three RBCs bound per cell, and, based on the previous analysis (Fig. 2), the optimal rate and final extent of fluorescence dequenching. For all four cell lines we determined the lag time preceding the onset of fusion, the initial rate of fusion, and the final extent of fusion. As seen in Fig. 3, the amount of HA expressed on the surface of the fibroblasts affected both the lag time preceding the onset of fusion and the initial rate of fusion. As the density of HA at the cell surface increased, the lag time preceding the onset of fusion decreased, and the initial rate of fusion increased. Nevertheless, under the conditions of this experiment, the final extent of fluorescent dequenching was similar (45 ± 4%) for all cell lines.

Variation in the Lag Time Preceding Fusion with HA Surface Density

We next wished to compare the lag phase preceding the onset of fusion among the set of cells that express HA at nine different defined surface densities (Table I). To normalize results from separate experiments, we used the cell line that expresses the lowest amount of HA (gp4/6) (Table I) as a reference. In each experiment, the lag time preceding the onset of fusion was measured for each cell line. This value was then expressed relative to the lag time observed (in the same experiment) for the gp4/6 cell line. We then plotted the average reciprocal lag time (1/lag) as a function of the relative density of HA in the plasma membrane. As seen in Fig. 4 *A*, as the density of HA on the cell surface increased, the lag time preceding the onset of fusion decreased significantly. Moreover, the dependence of the reciprocal lag time preceding the onset of fusion and HA surface density was clearly sigmoidal (Fig. 4 *A*).

The sigmoidal nature of the plot relating 1/lag to HA surface density is most pronounced in the region of HA density covered by the gp4/8 and HAb-2 cell lines (Fig. 4 *A*). To exclude the possibility that the observed steepness in this region is due to differences between the cell lines other than in HA surface density (although the two cell lines were derived from the same original transfection by

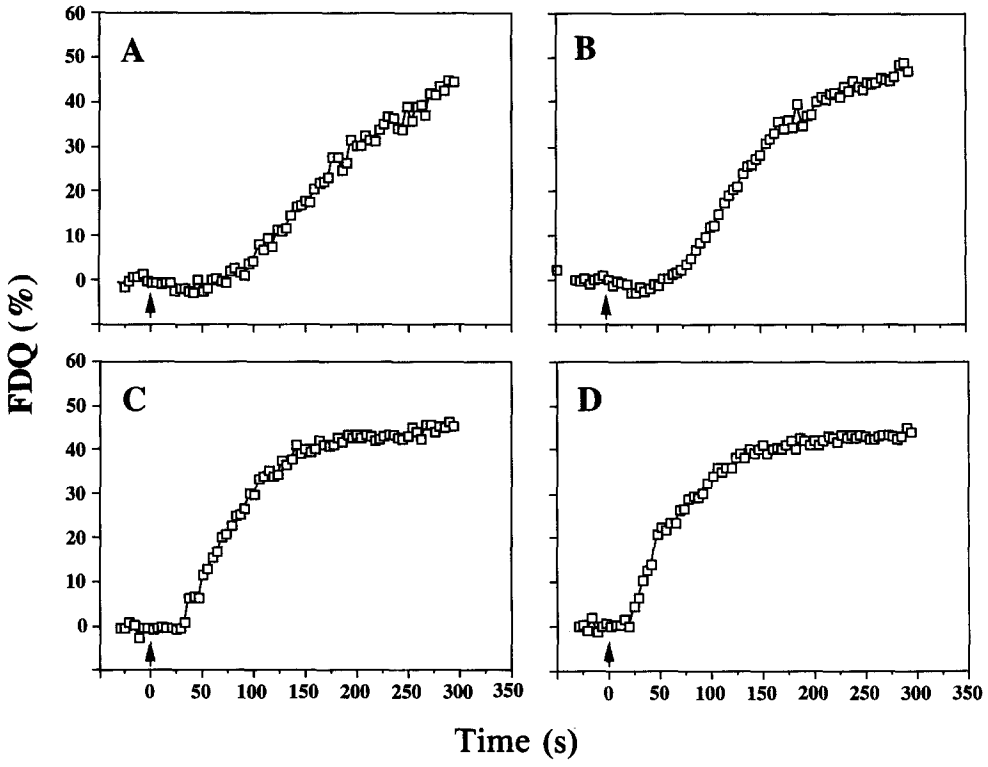

Figure 3. Fusion of R18-labeled RBCs with representative HA-expressing cell lines. R18-labeled RBCs (0.02%) were bound to each of the HA-expressing cell lines and assayed for fluorescence dequenching at 28° to 29°C as described in the legend to Fig. 2. Arrows indicate the time point ($t = 0$) at which the pH was lowered to 5.0. The cell lines shown are: (*A*) gp4/6, (*B*) gp4f, (*C*) HAb-2, and (*D*) 5 mM NaBut-induced HAb-2.

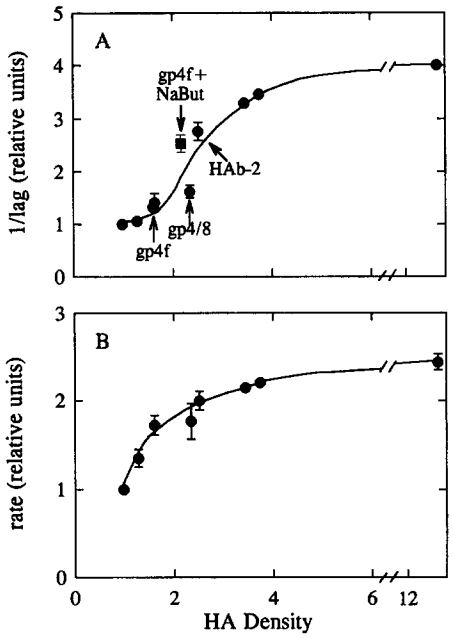

Figure 4. Effects of HA cell surface density on (*A*) the lag phase preceding and (*B*) the initial rate of fluorescence dequenching. The fusion of various HA-expressing cell lines with RBCs was analyzed by fluorescence dequenching as described in the legend to Fig. 2. HA density is expressed as trimers per μm^2 at the surface of the different cell lines. To correct for variations between sets of experiments, values for the reciprocal lag times and initial fusion rates were normalized relative to those for the gp4/6 cell line, which expresses the lowest amount of HA on its surface. Thus, 1/lag (s^{-1}) for the gp4/6 cell line was taken as 1 in *A*, and the initial rate of fusion (%/s) for the gp4/6 cell line was given the value 1 in *B*. The values for all of the other cell lines are expressed relative to those for the gp4/6 cells. (*A*) 1/lag vs HA density. Each point is the mean ± SEM of 5–15 determinations of the lag time for each cell line, using RBC concentrations of 0.02–0.03%. The cell lines whose surface density is given in Table I are depicted as closed circles. gp4f cells induced by 5 mM NaBut are depicted by a square; the level of increase in the density of HA at their surface was determined by surface biotinylation (see Materials and Methods). Two pairs of cell lines in the steep region of the curve, gp4f vs 5 mM NaBut-induced gp4f and gp4/8 vs HAb-2, are marked by arrows for ease of comparison. (*B*) Initial rate vs HA density. Each point is the mean ± SEM of six determinations. In *B* only rate data from experiments performed with 0.02% RBCs were analyzed, since the initial rate was dependent, to some degree, on the concentration of RBCs used.

identical procedures), we compared the lag phases for gp4f cells and for gp4f cells treated with 5 mM NaBut (to induce higher HA expression). As seen in Fig. 4 *A*, the sigmoidal nature of the curve, with a region of steep increase between the gp4/8 and HAb-2 cell lines, is retained. Furthermore, in a related experiment, fusion was monitored on the single cell level using video microscopy (Melikyan et al., 1995). In this study, when gp4f cells were treated with 5 mM NaBut, the lag phase before the onset of fusion, measured as the first detectable dye transfer, decreased by a factor of 1.6 (Melikyan, G., and F. Cohen, personal communication). This observed decrease is in the same range (1.9-fold) as that which we encountered using our fusion measurements.

Variation in the Initial Rate of Fusion with HA Surface Density

The relative initial rates of fusion as a function of relative HA surface density are depicted in Fig. 4 *B*. As noted previously (Fig. 3), a correlation was observed between HA surface density and the initial rate of fluorescence dequenching: cells that express more HA at their surface displayed a higher initial rate of fluorescence dequenching. However, in contrast to the sigmoidal dependence observed for the reciprocal lag time as a function of HA surface density (Fig. 4 *A*), the relationship between the initial rate of fluorescence dequenching and HA surface density displayed a hyperbolic, Michaelis-Menten–type dependence. The fact that the curve relating the initial rate of fusion to HA surface density reached saturation (Fig. 4 *B*) may reflect the opening of multiple independent fusion pores (Zimmerberg et al., 1994) and the attainment of a saturation density where the number of fusion pores in the region of contact with an attached RBC cannot increase further. Alternatively, the rate of migration of the lipid probe into the membrane of the HA-bearing cell may reach the diffusion limit for the flow of the lipid probe from an RBC into the underlying fibroblast.

Basis for the Sigmoidal Relationship between the Lag Time and HA Density

The sigmoidal dependence of the reciprocal lag time on HA surface density may suggest a cooperative process involving the concerted action of several HA trimers at an early stage of the fusion reaction. Several models can be envisioned to explain such cooperativity. One proposal was that HA cooperativity might stem from the aggregation of several HA trimers, before fusion, to generate a fusogenic complex (Blumenthal et al., 1991; Stegmann et al., 1990). If such an aggregation process were rate limiting, it could lead to a lag time before the onset of fusion. As described by Clague et al. (1991), the appropriate analysis to detect cooperativity in an aggregation process is by a log/log plot–plotting log (1/lag), which would be proportional to the rate of the process preceding fusion (in this case HA aggregation), against log [HA]. The slope of this plot would yield the minimum number of interacting units, in this case HA trimers. This can be exemplified by the simple case of obligate dimer formation: If "*A*" has to dimerize to enable a reaction, the chemical equation is $A + A \rightarrow A_2$, and the corresponding rate equation is $v = k[A]^2$. Therefore, $\log(v) = \log(k) + 2\log[A]$, and the slope of the resulting plot will be 2. A log/log analysis for 1/lag vs HA surface density is shown in Fig. 5. In this analysis, v = reciprocal lag time and $[A]$ = HA surface density. Leaving out the two extreme points, which clearly deviate from linearity, the resulting slope is 1.1 and does not show cooperativity. Hence, aggregation of HA trimers cannot be the rate-limiting step in an oligomerization reaction that gives rise to the lag time. However, this conclusion does not rule out cooperativity among HA trimers at some later step (after oligomerization has occurred). For example, if the fusion peptides of one HA trimer (already found in an aggregate) have inserted productively into the target cell membrane at a nascent fusion site, then this "primed" HA trimer could facilitate hydrophobic binding to the target

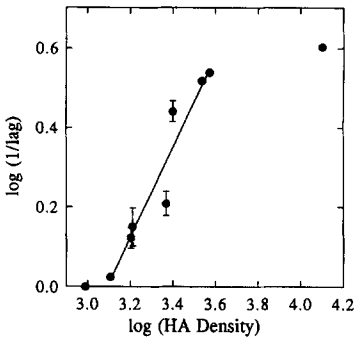

Figure 5. Log/log plot of reciprocal lag time vs HA surface density. The data were compiled from those shown in Fig. 4 *A*. HA density is expressed as trimers per μm^2 at the surfaces of the different cell lines depicted in Table I. The solid line shows a linear regression, excluding the two extreme points (cells expressing the lowest and highest HA concentrations, where deviations from linearity are likely to occur). The linear regression yields a slope of 1.1 with a correlation coefficient of 0.962.

membrane of fusion peptides from another trimer found in the same aggregate (see Discussion). Such a cooperative process can be modeled as a ligand binding to a binding site. In such a model for HA-induced membrane fusion, the "ligand" is the HA trimer and the "binding site" is the nascent fusion site on the target membrane. The possibility of cooperative binding of a ligand (HA trimer) to a binding site (fusion site) can then be evaluated by a Hill plot, a plot typically used to analyze systems that display cooperative binding (Levitzki, 1978).

Fig. 6 depicts a Hill plot analysis of the dependence of the reciprocal lag time on HA surface density. This plot clearly indicates positive cooperativity (characterized by $n_H > 1$). Considering that at the low and high extremes of concentration the Hill plot deviates from linearity, and its slope approaches 1 (Levitzki, 1978), we performed linear regression analyses of the region of midsaturation. In Fig. 6 *A*, we present a conservative analysis, which excluded the gp4/6 and gp4/10 cells on the low end of HA surface density and 5 mM NaBut-induced HAb-2 cells on the high end. A linear regression of the included points (*solid line*) yielded a slope at midsaturation, n_H, equal to 2.8. This result suggests the participation of at least three HA trimers in a cooperative process (Fig. 6 *A*). If the next two cell lines at the low end of HA expression, gp4f and gp4/9, are also excluded, then n_H equals 3.7 (Fig. 6 *B*). The latter analysis (Fig. 6 *B*) suggests that a minimum of four HA trimers is required to initiate a fusion event.

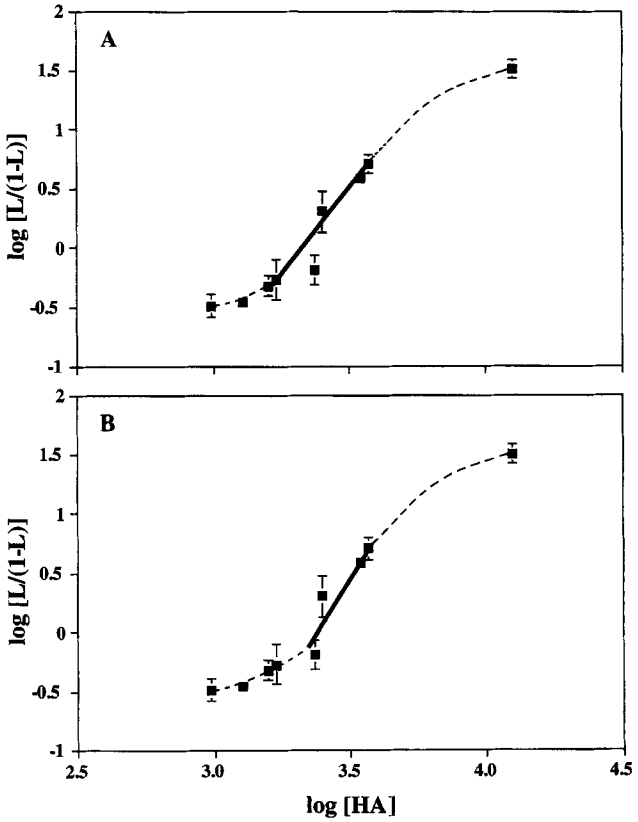

Figure 6. Hill plot of the dependence of the reciprocal lag time preceding the onset of fusion on HA surface density. The data were compiled from those shown in Fig. 4 *A*. The 1/lag values were recalibrated such that the highest value at saturation is 1, to make them equal to the values of the saturation function (see detailed explanation in the Materials and Methods section). The 1/lag value at saturation was defined by plotting 1/lag of the three points at the highest surface density vs 1/HA density and extrapolating to infinite density (1/HA density = 0). This was repeated iteratively three times until the extrapolated value changed by less than 1%. Log $[L/(1-L)]$ is plotted against log [HA], where L is 1/lag time, and [HA] is the density of HA trimers (in trimers per μm^2) at the surface of the different cell lines (depicted in Table I). The solid lines show linear regression fits; the points excluded from the fits (because they are either at very high or very low occupancies, where the Hill plot deviates from linearity) are connected by dashed lines. In *A*, the first two points and the last point were omitted from the linear regression (*solid line*). From this linear regression, the slope at midsaturation yields $n_H = 2.83$, with a correlation coefficient of 0.998. In *B*, the first four points and the last point were omitted from the linear regression. From this linear regression (*solid line*), the slope at midsaturation yields $n_H = 3.68$, with a correlation coefficient of 0.999. The slope of a separate linear regression of the first four points = 0.93, with a correlation coefficient of 0.999.

Discussion

In this study we addressed two basic questions: does membrane fusion mediated by the influenza virus HA require the cooperative action of several HA trimers? And, if so, what is the minimum number of trimers required? Our approach was to compare the fusion reactions of cell lines that express increasing defined amounts of HA on their surface. Using this approach we observed that the curve relating the lag phase preceding the onset of fusion and HA surface density was sigmoidal (Fig. 4 *A*). In contrast, the curve relating the initial rate of fusion (after the lag time) and HA surface density displayed a Michaelis-Menten–type profile (Fig. 4 *B*). This indicates that a process (or processes) preceding fusion needs to occur before fusion can commence, and that the rate of this "activation" process (reflected in the reciprocal lag time) depends cooperatively on HA density. The initial rate of fusion is measured at the end of the lag period, after the activation is

complete. The initial rate should thus be proportional to the concentration of the active fusogenic entities already formed and is not expected to reflect the cooperativity of the activation rate.

To test whether the basis for the observed sigmoidicity (Fig. 4 *A*) is aggregation of HA trimers, we analyzed our data according to a log/log plot, as was done previously by Clague et al. (1991). In agreement with their findings, our analysis (Fig. 5) indicated that rate-limiting association of several HA trimers (e.g., to form a fusogenic complex) is not a cooperative process. This analysis does not preclude, however, the possibilities that HA aggregation occurs during the lag phase or that HA aggregation is required for fusion. To explore further the possibility that a cooperative process occurs during the lag phase, we used a Hill plot analysis (Fig. 6), an analysis used routinely for systems that display cooperative binding. Such an analysis is justified for any model that involves the binding of several ligand molecules to an entity capable of binding more than one molecule of ligand. In our case, the ligand is an HA trimer, and the multimeric binding entity is the nascent fusion site on the target membrane. This analysis (Fig. 6, *A* and *B*) gave a clear demonstration of positive cooperativity and yielded n_H values of 2.8 or 3.7. Our results therefore indicate that a minimum of three, and likely a minimum of four, HA trimers is required to initiate a fusion reaction. Our findings therefore provide the first direct experimental evidence for cooperativity in HA-mediated fusion, as suggested previously (Bentz, 1992; Bentz et al., 1990; Blumenthal et al., 1991; Doms and Helenius, 1986; Ellens et al., 1990; Guy et al., 1992; Kemble et al., 1994; Morris et al., 1989; Stegmann et al., 1990; White, 1994).

As discussed above, the cooperativity observed for the lag phase is not due to rate-limiting aggregation of HA trimers. What then is the basis for HA cooperativity? Essentially, any model where the interaction of one HA trimer with the nascent fusion site facilitates the interaction of additional HAs with the target site can give rise to the sigmoidal dependence of the rate of the process(es) occurring during the lag time on HA density. If limited aggregates (complexes) of HA trimers form early in the lag phase (as suggested by the observation that HA aggregation is not the rate-limiting step), a likely model is that insertion of the hydrophobic fusion peptides of one HA trimer in the aggregate into the nascent fusion site facilitates the insertion of the fusion peptides of neighboring HAs residing in the same complex. At this stage, the HA aggregate interacting with the target membrane can be envisioned as a "prefusion pore" complex, somewhere on the way to forming an active fusion pore.

The ability of the fusion peptides to interact productively with the fusion site likely involves changes in HA structure (Bullough et al., 1994; Carr and Kim, 1993; Hughson, 1995) and orientation vis-a-vis the fusing membranes (Tatulian et al., 1995; Wharton et al., 1995). It may also involve changes in HA lateral (Gutman et al., 1993) and rotational (Junankar and Cherry, 1986) mobility. Several recent studies have addressed the interaction of the HA fusion peptide with target membranes using photoactivatable phospholipid cross-linking reagents (Brunner et al., 1991; Harter et al., 1989; Pak et al., 1994; Stegmann et al., 1991). Although one study, using X:31 influenza virus (H3 subtype) and liposomes, concluded that hydrophobic interaction of HA with the target membrane is quantitatively complete in the beginning of the lag phase (Stegmann et al., 1991), other studies, on the interaction of both X:31 and PR8 (H1 subtype) viruses with either liposomes or RBCs, concluded that there is significantly enhanced fusion peptide labeling during the lag phase (Brunner et al., 1991; Pak et al., 1994; Tsurudome et al., 1992). Whether all of the fusion peptides that participate in fusion bind to the target membranes at the beginning of, during, or at the end of the lag phase (which may depend, in part, upon the virus strain) (Ellens et al., 1990; Gutman et al., 1993; Puri et al., 1990), the collective data suggest that during the lag phase there may be qualitative changes (see below) leading to productive (and cooperative) interaction of fusion peptides with the target site.

Productive and cooperative interaction of HA fusion peptides with the target site likely requires that the fusion peptide has a specific sequence, secondary structure, and angle of interaction with the target membrane (Brasseur et al., 1990; Rafalski et al., 1990, 1991; Stegmann et al., 1995; Gething et al., 1986; Danieli, T., unpublished observations). This idea is supported by the observations that a site-specific mutant in the HA fusion peptide (gly1 to glu) displays no fusion activity, although it is capable of binding to target liposomes (Gething et al., 1986), and that only certain amino acids are allowed at position 1 of the fusion peptide (Qiao, H., and J. White, manuscript in preparation; Steinhauer et al., 1995).

Formally, our experiments do not reveal which stage of the fusion process (e.g., hemifusion, fusion pore opening, or fusion pore dilation) is cooperative with respect to HA trimers. However, since the fusion assay we used monitored the onset of outer leaflet lipid mixing, our results suggest that an early stage of the fusion process, perhaps formation of a hemifusion intermediate (Kemble et al., 1994; White, 1994), involves a cluster of three to four HA trimers. Support for this hypothesis is the observation that a functional and exposed fusion peptide is required to reach the hemifusion state (Godley et al., 1992; Guy et al., 1992; Kemble et al., 1992; Danieli, T., unpublished observations; Qiao, H., and J. White, manuscript in preparation).

The number that we have arrived at for the minimum number of HA trimers required to initiate a fusion event, three to four trimers, is in good agreement with estimates (4–10 trimers) based on the initial conductance of the HA fusion pore (Spruce et al., 1991) and on theoretical considerations (Bentz, 1992). If the nascent fusion pore is surrounded by three to four HA trimers, then there might be a ring of, minimally, 9 or 12 HA transmembrane helices around the initial pore. Given the recently appreciated role for the HA transmembrane domain in the fusion process (Kemble et al., 1994; Melikyan et al., 1995), a bundle of transmembrane helices could be a key structural element of the HA fusion pore (Guy et al., 1992). It is not yet known whether final irreversible dilation of the pore (Melikyan et al., 1993*a*,*b*; Spruce et al., 1991; Tse et al., 1993; Zimmerberg et al., 1994) involves recruitment of additional HA trimers.

In conclusion, our results strongly suggest that HA-mediated fusion requires the concerted action of, minimally, three to four HA trimers. Recent studies of other enveloped vi-

ruses, for example human immunodeficiency virus (HIV), Semliki Forest virus (SFV), and vesicular stomatitis virus (VSV), have provided hints that other viral fusion reactions require higher order clusters of their viral membrane fusion proteins (Blumenthal et al., 1991; Bron et al., 1993; Brown et al., 1988; Clague et al., 1991; Freed et al., 1992; Gaudin et al., 1993; Lanzrein et al., 1993; Layne et al., 1990). We therefore suggest that all enveloped viruses require cooperative interactions among their membrane fusion proteins to promote fusion. Furthermore, cell–cell fusion reactions (Blobel et al., 1992) and exocytic fusion reactions (Lindau and Almers, 1995; Monck and Fernandez, 1992; Zimmerberg et al., 1993), as well as other intracellular fusion reactions (Sollner et al., 1993), may also involve cooperative interactions among sets of components that constitute their respective fusion machines.

We thank Eduardo Almeida for help with confocal microscopy, Tamar Manor and Orit Gutman for fluorescence measurements, and Fred Cohen for sharing unpublished results and for helpful discussions.

The work was supported by a grant from the National Institutes of Health (NIH) (AI22470) to J.M. White and by a grant from the United States–Israel Binational Science Foundation (91-00041) (Jerusalem, Israel), to Y.I. Henis. T. Danieli was supported, in part, by a predoctoral fellowship from the American Association of University Women. S.L. Pelletier was supported by an NIH training grant (T32 CA09109).

Received for publication 18 November 1995 and in revised form 23 January 1996.

References

Axelrod, D., D.E. Koppel, J. Schlessinger, E.L. Elson, and W.W. Webb. 1976. Mobility measurement by analysis of fluorescence photobleaching recovery kinetics. *Biophys. J.* 16:1055–1069.

Bennett, M.K., and R.H. Scheller. 1994. A molecular description of synaptic vesicle membrane trafficking. *Annu. Rev. Biochem.* 63:63–100.

Bentz, J. 1992. Intermediates and kinetics of membrane fusion. *Biophys. J.* 63: 448–459.

Bentz, J., H. Ellens, and D. Alford. 1990. An architecture for the fusion site of influenza hemagglutinin. *FEBS Lett.* 276:1–5.

Benveniste, M., E. Livneh, J. Schlessinger, and Z. Kam. 1988. Overexpression of epidermal growth factor receptor in NIH-3T3–transfected cells slows its lateral diffusion and rate of endocytosis. *J. Cell Biol.* 106:1903–1909.

Blobel, C.P., T.G. Wolfsberg, C.W. Turck, D.G. Myles, P. Primakoff, and J.M. White. 1992. A potential fusion peptide and an integrin ligand domain in a protein active in sperm-egg fusion. *Nature (Lond.).* 356:248–252.

Blumenthal, R., C. Schoch, A. Puri, and M. J. Clague. 1991. A dissection of steps leading to viral envelope protein-mediated membrane fusion. *In* Calcium Entry and Action at Presynaptic Nerve Terminal. Vol. 635. E.F. Stanley, M.C. Nowycky, and D.J. Triggle, editors. New York Academy of Sciences, New York. 285–297.

Brasseur, R., M. Vandenbranden, B. Cornet, A. Burny, and J.-M. Ruysschaert. 1990. Orientation into the lipid bilayer of an asymmetric amphipathic helical peptide located at the N-terminus of viral fusion proteins. *Biochim. Biophys. Acta.* 1029:267–273.

Bron, R., J.M. Wahlberg, H. Garoff, and J. Wilschut. 1993. Membrane fusion of Semliki forest virus in a model system: correlation between fusion kinetics and structural changes in the envelope glycoprotein. *EMBO (Eur. Mol. Biol. Organ.) J.* 12:693–701.

Brown, J.C., W.W. Newcomb, and S. Lawrenz-Smith. 1988. pH-dependent accumulation of the Vesicular stomatitis virus glycoprotein at the ends of intact virions. *Virology.* 167:625–629.

Brunner, J., C. Zugliani, and R. Mischler. 1991. Fusion activity of influenza virus PR8/34 correlates with a temperature-induced conformational change within the hemagglutinin ectodomain detected by photochemical labeling. *Biochemistry.* 30:2432–2438.

Bullough, P.A., F.M. Hughson, J.J. Skehel, and D.C. Wiley. 1994. Structure of influenza haemagglutinin at the pH of membrane fusion. *Nature (Lond.).* 371:37–43.

Carr, C.M., and P.S. Kim. 1993. A spring-loaded mechanism for the conformational change of influenza hemagglutinin. *Cell.* 73:823–832.

Clague, M.J., C. Schoch, and R. Blumenthal. 1991. Delay time for influenza virus hemagglutinin-induced membrane fusion depends on hemagglutinin surface density. *J. Virol.* 65:2402–2407.

Cooper, J.A., E.L. Buhle, S.B. Walker, T.Y. Tsong, and T.D. Pollard. 1983. Kinetic evidence for a monomer activation step in actin polymerization. *Biochemistry.* 22:2193–2202.

Doms, R.W., and A. Helenius. 1986. Quaternary structure of influenza virus hemagglutinin after acid treatment. *J. Virol.* 60:833–839.

Doxsey, S., J. Sambrook, A. Helenius, and J. White. 1985. An efficient method for introducing macromolecules into living cells. *J. Cell Biol.* 101:19–27.

Ellens, H., J. Bentz, D. Mason, F. Zhang, and J.M. White. 1990. Fusion of influenza hemagglutinin-expressing fibroblasts with glycophorin-bearing liposomes: role of hemagglutinin surface density. *Biochemistry.* 29:9697–9707.

Ferro-Novick, S., and R. Jahn. 1994. Vesicle fusion from yeast to man. *Nature (Lond.).* 370:191–193.

Fire, E., D.E. Zwart, M.G. Roth, and Y.I. Henis. 1991. Evidence from lateral mobility studies for dynamic interactions of a mutant influenza hemagglutinin with coated pits. *J. Cell Biol.* 115:1585–1594.

Freed, E.O., E.L. Delwart, G.L. Buchschacher, and A.T. Panganiban. 1992. A mutation in the human immunodeficiency virus type 1 transmembrane glycoprotein gp41 dominantly interferes with fusion and infectivity. *Proc. Natl. Acad. Sci. USA.* 89:70–74.

Gaudin, Y., R.W.H. Ruigrok, M. Knossow, and A. Flamand. 1993. Low-pH conformational changes of rabies virus glycoprotein and their role in membrane fusion. *J. Virol.* 67:1365–1372.

Gething, M.-J., R.W. Doms, D. York, and J.M. White. 1986. Studies on the mechanism of membrane fusion: site-specific mutagenesis of the hemagglutinin of influenza virus. *J. Cell Biol.* 102:11–23.

Godley, L., J. Pfeifer, D. Steinhauer, B. Ely, G. Shaw, R. Kaufmann, E. Suchanek, C. Pabo, J.J. Skehel, D.C. Wiley, and S. Wharton. 1992. Introduction of intersubunit disulfide bonds in the membrane-distal region of the influenza hemagglutinin abolishes membrane fusion activity. *Cell.* 68:635–645.

Gutman, O., T. Danieli, J.M. White, and Y.I. Henis. 1993. Effects of exposure to low pH on the lateral mobility of influenza hemagglutinin expressed at the cell surface. *Biochemistry.* 32:101–106.

Guy, H.R., S.R. Durell, C. Schoch, and R. Blumenthal. 1992. Analyzing the fusion process of influenza hemagglutinin by mutagenesis and molecular modeling. *Biophys. J.* 62:95–97.

Harter, C., P. James, T. Bächi, G. Semenza, and J. Brunner. 1989. Hydrophobic binding of the ectodomain of influenza hemagglutinin to membranes occurs through the "fusion peptide." *J. Biol. Chem.* 264:6459–6464.

Henis, Y.I., and O. Gutman. 1983. Lateral diffusion and patch formation of H-2K^k antigens on mouse spleen lymphocytes. *Biochim. Biophys. Acta.* 762: 281–288.

Hughson, F.M. 1995. Structural characterization of viral fusion proteins. *Curr. Biol.* 5:265–274.

Junankar, P.R., and R.J. Cherry. 1986. Temperature and pH dependence of the haemolytic activity of influenza virus and of the rotational mobility of the spike glycoproteins. *Biochim. Biophys. Acta.* 854:198–206.

Kemble, G.W., D.L. Bodian, J. Rosé, I.A. Wilson, and J.M. White. 1992. Intermonomer disulfide bonds impair the fusion activity of influenza virus hemagglutinin. *J. Virol.* 66:4940–4950.

Kemble, G.W., Y. Henis, and J.M. White. 1993. GPI- and transmembrane-anchored influenza hemagglutinin differ in structure and receptor binding activity. *J. Cell Biol.* 122:1253–1265.

Kemble, G.W., T. Danieli, and J.M. White. 1994. Lipid-anchored influenza hemagglutinin promotes hemifusion, not complete fusion. *Cell.* 76:383–391.

Koppel, D.E., D. Axelrod, J. Schlessinger, E.L. Elson, and W.W. Webb. 1976. Dynamics of fluorescent marker concentration as a probe of mobility. *Biophys. J.* 16:1315–1329.

Lanzrein, M., N. Kasermann, R. Weingart, and C. Kempf. 1993. Early events of Semliki forest virus-induced cell-cell fusion. *Virology.* 196:541–547.

Layne, S.P., M.J. Merges, M. Dembo, J.L. Spouge, and P.L. Nara. 1990. HIV requires multiple gp120 molecules for CD4-mediated infection. *Nature (Lond.).* 346:277–279.

Levitzki, A. 1978. Quantitative aspects of allosteric mechanisms. *In* Molecular Biology, Biochemistry and Biophysics. Vol. 28. A. Kleinzeller, G.F. Springer, and H.G. Wittmann, editors. Springer Verlag, Berlin. 1–106.

Lindau, M., and W. Almers. 1995. Structure and function of fusion pores in exocytosis and ectoplasmic membrane fusion. *Curr. Opin. Cell Biol.* 7:509–517.

Melikyan, G.B., W.D. Niles, and F.S. Cohen. 1993*a*. Influenza virus hemagglutinin-induced cell-planar bilayer fusion: quantitative dissection of fusion pore kinetics into stages. *J. Gen. Physiol.* 102:1151–1170.

Melikyan, G.B., W.D. Niles, M.E. Peeples, and F.S. Cohen. 1993*b*. Influenza hemagglutinin-mediated fusion pores connecting cells to planar membranes: flickering to final expansion. *J. Gen. Physiol.* 102:1131–1149.

Melikyan, G.B., J.M. White, and F.S. Cohen. 1995. GPI-anchored influenza hemagglutinin induces hemifusion to both red blood cell and planar bilayer membranes. *J. Cell Biol.* 131:679–691.

Monck, J.R., and J.M. Fernandez. 1992. The exocytotic fusion pore. *J. Cell Biol.* 119:1395–1404.

Morris, S., D. Sarkar, J. White, and R. Blumenthal. 1989. Kinetics of pH-dependent fusion between 3T3 fibroblasts expressing influenza hemagglutinin and red blood cells. Measurement by dequenching of fluorescence. *J. Biol. Chem.* 264:3972–3978.

Pak, C.C., M. Krumbiegel, R. Blumenthal, and Y. Raviv. 1994. Detection of influenza hemagglutinin interaction with biological membranes by photosensitized activation of [^{125}I]Iodonapthylazide. *J. Biol. Chem.* 269:14614–14619.

Petersen, N.O., S. Felder, and E.L. Elson. 1986. Measurement of lateral diffu-

sion by fluorescence photobleaching recovery. *In* Handbook of Experimental Immunology. D.M. Weir, L.A. Herzenberg, C.C. Blackwell, and L.A. Herzenberg, editors. Blackwell Scientific Publications, Ltd., Edinburgh. 24.1–24.23.

Pryer, N.K., L.J. Wuestehube, and R. Schekman. 1992. Vesicle-mediated protein sorting. *Annu. Rev. Biochem.* 61:471–516.

Puri, A., F.P. Booy, R.W. Doms, J.M. White, and R. Blumenthal. 1990. Conformational changes and fusion activity of influenza virus hemagglutinin of the H2 and H3 subtypes: effects of acid pretreatment. *J. Virol.* 64:3824–3832.

Rafalski, M., J.D. Lear, and W.F. DeGrado. 1990. Phospholipid interactions of synthetic fusion peptides representing the N-terminus of HIV gp41. *Biochemistry.* 29:7917–7922.

Rafalski, M., A. Ortiz, A. Rockwell, L.C. van Ginkel, J.D. Lear, W.F. DeGrado, and J. Wilschut. 1991. Membrane fusion activity of the influenza virus hemagglutinin: interaction of HA2 N-terminal peptides with phospholipid vesicles. *Biochemistry.* 30:10211–10220.

Rothman, J.E. 1994. Mechanisms of intracellular protein transport. *Nature (Lond.).* 372:55–63.

Sambrook, J., L. Rodgers, J. White, and M.J. Gething. 1985. Lines of BPV-transformed murine cells that constitutively express influenza virus hemagglutinin. *EMBO (Eur. Mol. Biol. Organ.) J.* 4:91–103.

Sollner, T., S.W. Whiteheart, M. Brunner, H. Erdjument-Bromage, S. Geromanos, P. Tempst, and J.E. Rothman. 1993. SNAP receptors implicated in vesicle targeting and fusion. *Nature (Lond.).* 362:318–324.

Spruce, A.E., A. Iwata, J.M. White, and W. Almers. 1989. Patch clamp studies of single cell-fusion events mediated by a viral fusion protein. *Nature (Lond.).* 342:555–558.

Spruce, A.E., A. Iwata, and W. Almers. 1991. The first milliseconds of the pore formed by a fusogenic viral envelope protein during membrane fusion. *Proc. Natl. Acad. Sci. USA.* 88:3623–3627.

Stegmann, T., and A. Helenius. 1993. Influenza virus fusion: from models toward a mechanism. *In* Viral Fusion Mechanisms. J. Bentz, editor. CRC Press, Inc., Boca Raton, FL. 89–111.

Stegmann, T., R.W. Doms, and A. Helenius. 1989. Protein-mediated membrane fusion. *Annu. Rev. Biophys. Biophys. Chem.* 18:187–211.

Stegmann, T., J.M. White, and A. Helenius. 1990. Intermediates in influenza-induced membrane fusion. *EMBO (Eur. Mol. Biol. Organ.) J.* 9:4231–4241.

Stegmann, T., J.M. Delfino, F.M. Richards, and A. Helenius. 1991. The HA2 subunit of influenza hemagglutinin inserts into the target membrane prior to fusion. *J. Biol. Chem.* 266:18404–18410.

Stegmann, T., I. Bartoldus, and J. Zumbrunn. 1995. Influenza hemagglutinin-mediated membrane fusion: influence of receptor binding on the lag phase preceding fusion. *Biochemistry.* 34:1825–1832.

Steinhauer, D.A., S.A. Wharton, J.J. Skehel, and D.C. Wiley. 1995. Studies of membrane fusion activities of fusion peptide mutants of influenza virus hemagglutinin. *J. Virol.* 69:6643–6651.

Südhof, T.C., P. De Camilli, H. Niemann, and R. Jahn. 1993. Membrane fusion machinery: insights from synaptic proteins. *Cell.* 75:1–4.

Tatulian, S.A., P. Hinterdorfer, G. Baber, and L.K. Tamm. 1995. Influenza hemagglutinin assumes a tilted conformation during membrane fusion as determined by attenuated total reflection FTIR spectroscopy. *EMBO (Eur. Mol. Biol. Organ.) J.* 14:5514–5523.

Tse, F.W., A. Iwata, and W. Almers. 1993. Membrane flux through the pore formed by a fusogenic viral envelope protein during cell fusion. *J. Cell Biol.* 121:543–552.

Tsurudome, M., R. Glück, R. Graf, R. Falchetto, U. Schaller, and J. Brunner. 1992. Lipid interactions of the hemagglutinin HA2 NH_2-terminal segment during influenza virus-induced membrane fusion. *J. Biol. Chem.* 267:20225–20232.

Wharton, S.A., L.J. Calder, R.W.H. Ruigrok, J.J. Skehel, D.A. Steinhauer, and D.C. Wiley. 1995. Electron microscopy of antibody complexes of influenza virus hemagglutinin in the fusion pH conformation. *EMBO (Eur. Mol. Biol. Organ.) J.* 14:240–246.

White, J.M. 1992. Membrane fusion. *Science (Wash. DC).* 258:917–924.

White, J.M. 1994. Fusion of influenza virus in endosomes: role of the hemagglutinin. *In* Cellular Receptors for Animal Viruses. E. Wimmer, editor. Cold Spring Harbor Laboratory, Cold Spring Harbor, NY. pp. 281–301.

Wiley, D.C., and J.J. Skehel. 1987. The structure and function of the hemagglutinin membrane glycoprotein of influenza virus. *Annu. Rev. Biochem.* 56:365–394.

Zimmerberg, J., S.S. Vogel, and L.V. Chernomordik. 1993. Mechanisms of membrane fusion. *Annu. Rev. Biophys. Biomol. Struct.* 22:433–466.

Zimmerberg, J., R. Blumenthal, D.P. Sarkar, M. Curran, and S.J. Morris. 1994. Restricted movement of lipid and aqueous dyes through pores formed by influenza hemagglutinin during cell fusion. *J. Cell Biol.* 127:1885–1894.